Sequence Stratigraphy and Diagenetic Controls on Reservoir Quality of the Carboniferous Marar and Assedjefar Formations Murzuq Basin, SW Libya

Mohammed Bukar[1], Fauziyah Ahmad Rufai[2] and Asabe Yahaya Kuku[1]

[1]Department of Geology, University of Maiduguri, Nigeria.
[2]Department of Geology, Modibbo Adama University of Technology Yola, Nigeria.

Abstract:

Background: *This study involves analysis of well logs and thin section studies from outcrop samples to produce a sequence stratigraphy and diagenetic interpretation of the Carboniferous Marar and lower Assedjefar Formations in the Murzuq Basin, SW Libya. Well log data and i8 thin sections prepared from outcrop samples were used. Petrel Schlumberger software was used for the sequence stratigraphic construction and Petrographic and Scanning Electron Microscope (SEM) were used for the diagenetic studies. A total of 200 points were counted per slide. Chronostratigraphic panels roughly in N-S and E-W orientations were constructed using log signatures. The Marar Formation is on average 400m thick, and can be divided into 4 upward coarsening sequences, SM-1, SM-2, SM-3, and SM-4.The lower Assedjefar is not fully covered assigned to one sequence (SA-1). Three sandstone units A, B and C were examined. Sandstone Unit A is an incised valley of the lowstand systems tract (LST) of sequence SA-1 in Assedjefar Formation and Units B and C are incised valley fills of LST of sequence SM-4 in Marar Formation. Sandstone unit B is at distal while unit C is at proximal location with influence of meteoric water digestion. They showed different compositional and diagenetic character. Sandstone units A and B are arkoses, fine grained, well-sorted, with abundant mud clasts, pore-filling and grain replacing calcite cements and low porosity (average of 5%). The sandstone Unit C is a quartz arenite, fine grained, and very well sorted, with high primary and dissolution porosity (average of 15%) and booklets of kaolinite. The sandstone in Units A and B have relatively poor reservoir quality while the sandstone in Unit C is a good reservoir.*

Keywords*: Murzuq. diagenesis, sequence stratigraphy, reservoir quality, meteoric water.*

I.   Introduction:

Sequence stratigraphy has been used over the years to subdivide the sedimentary record into sequences and component units. This has been used to interpret, describe and predict temporal and spatial distribution of depositional facies and their geometries (e.g. Haq *et al*., 1987; Van Wagoner *et al*., 1990). The deposition of sediments in a sequence is mainly controlled by relative sea level change, rate of sediment supply and basin and slope geometries. This interplay of sea level change and sediment supply affects pore water chemistry, organic matter content and type, amount of detrital sediment influx and type, and resident time of sediments under particular chemical condition (Morad *et al*., 2000; Ketzer et al., 2003). These factors have control on the amount and type of detrital clays and all the digenetic changes sediment undergoes after burial which include mechanical compaction, dissolutions, precipitation of cements (silica, pyrite, calcite, iron, dolomite etc) and development of authigenic clays of various types (kaolinite, illite, zeolite, smectite, etc). Cement precipitations and clay distributions forms barriers for fluid flow and dissolutions (mainly by meteoric water) creates pores for fluid accommodation and migration path way.

Combining sequence stratigraphy and diagenetic studies allow a better understanding of the controls on diagenesis and prediction of reservoir distribution. The study area is located in the northwestern part of Murzuq Basin (Fig. 1) Southwest of Libya. The stratigraphic interval studied is the Early Carboniferous Marar formation and lower part of the Assedjefar formation both about 500 m thick which were deposited in deltaic environment.
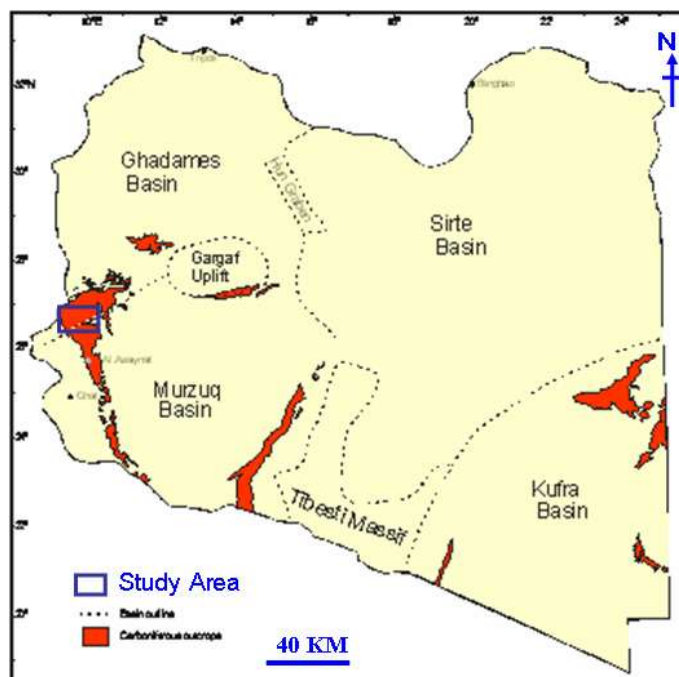

Figure 1: Location map of Murzuq Basin showing the study area where outcrop samples were collected. Well locations and outcrop locations are given in figure 3.

II. Geological Setting of the Study Area

The Murzuq Basin is a huge Paleozoic cratonic basin located on the North African Saharan platform, SW of Libya (Fig. 1). The basin contains up to 4000m of Paleozoic marine deposits truncated by Mesozoic to Quaternary continental deposits (Davidson *et al*., 2000; Echikh and Sola, 2000 and Hallet, 2002). The present day basin is triangular to sub circular in shape and extends southward towards the Northern Republic of Niger where referred to as Djado Basin. The present day borders of the Murzuq basin are defined by erosion resulting from multi-phased tectonic uplifts, the flanks comprising the Tihemboka High to the west, the Tibesti High to the east and the Gargaf/Atshan Uplift to the north. These uplifts were generated by various tectonic events ranging from mid-Paleozoic through to Tertiary times, but the main uplift took place during mid Cretaceous (Austrian) and early Tertiary (Alpine) movements (Davidson *et al*., 2000). During this time sedimentation were thought to be mainly controlled by the NW-SE trending Tripoli-Tibesti Uplift (Keitzsch, 1971), which extend across north-eastern part of the present day basin.

Structural Setting

Detailed description of the present day structural configuration of the Murzuq basin was provided by Echikh *et al*., (2000) and Echikh and Sola (2000). The major tectonic elements within the basin include the Tirine High separating the Awaynat and Awbari troughs and the Traghan High between the Awbari and Dor Al Gussah troughs. In general the density and structural complexity increase from the southern, more stable parts of the basin towards the north eastern and north western portions. The most intensely faulted areas are located over the Tiririne and Traghan Highs.

Tiririne High

This is an asymmetrical NW to SE structure that is downfaulted to the west. The north westernmost part of the high is marked by the regional Tumarolin wrench fault which can be identified on the surface, trending in NNE SSW direction and extends from the Atshan High southwards over a distance of more than 250 km along the margins of the Tihemboka Arch. The fault shows about 20 km of right-lateral displacement of Carboniferous units in exposure close to the Tihemboka Arch (Echikh and Sola, 2000). In the Atshan area, the Tumorolin master fault is associated with en echelon fold pattern reflecting oblique compression. A positive flower structure associated with this fault, originated during the transpressional Hercynian movement was interpreted from a seismic section by Echick and Sola. The southern part of Tiririne is the most intensively faulted and complicated, characterized by the presence of a large local anticline with an aerial extent of 120 km^2. Two regional wrench faults, the Wadi Zalaylan and Birtazit, cut across this area following the same trend with the Tumarolin wrench fault.

Traghan High

Several fault sets affected the Traghan high which dips westward with trends changing from SE-NW to SW-NE in its northern part. Different structural styles ranging from simple and fault bounded anticlines produced during the Hercynian tectonic, flat local structures at the Ordovician /Silurian level and vertical closure upward in Mesozoic section forming major hydrocarbon traps have been reported by oil companies (Echikh and Sola, 2000).

Stratigraphy and Tectonic Evolution
Cambrians

The first sediments to be deposited in the basin belong to the Cambrian Hasawanah Formation (Fig. 2). A basal conglomerate has been recorded, but most of the formation comprises medium to very coarse grained, quartzitic sandstone. The environment of deposition passed from fluvial at the base to shallow marine at the top. Sediment supply was from the south, with the sea transgressing from the north. A section of 150 m is exposed in the Tikiumit area but only the upper 50-60 m is visible further the south (Hallet, 2002). Ordovician

Overlying the Hasanawa Formation is the Ordovician Hawaz Formation separated by major unconformity. The Hawaz Formation consists of fine to medium-grained sandstone, with subordinate siltstone and shale. This section has been described by Vos (1981), who suggested that the sediments were deposited in a fan delta complex which prograded across the Gargaf Uplift in a northernly direction. The Ash Shabiyat Formation is probably the lateral equivalent of the Hawaz Formation on the Tihemboka High shales of the upper Ordovician Melaz Shuqran Formation which has been dated to the Ashgill (Abugares and Remaekers, 1993).

The Ordovician Mamuniyat Formation (Fig. 2) overlies the Hawaz formation transitionally. The uppermost part of this Formation forms the primary hydrocarbon reservoir in the basin. The reservoir properties and characteristics of this Formation are described below in many literatures It comprises 100-140 m of massive, cross bedded sandstones representing a basal lowstand system, The palynological evidence suggests a Caradocian age for the Mamuniyat formation whilst brachiopod evidence indicates an Ashgillian age (Hallet, 2002).

The sandstone is typically quartzitic, fine to medium-grained, and fairly well sorted. Several different facies can be recognized within the Mamuniyat formation, although most can be assigned to a high energy deltaic to marine environment of deposition. The Mamuniyat and the underlying Melaz Shuqran formations were deposited at a time of glaciations over North Africa, which lay along the margins of Gondwana. The evidence for this is the direct evidence of glaciations observed by (Davidson et al., 2000), the presence of small dropstones in the Melaz Shuqran shale and the occurrence of interpreted ice striations on the bedding planes within the Mamuniyat Formation. Mamuniyat Formation may contain a series of deeply incised erosional channels filled with fluvio-glacial sediments (Smart, 2000).
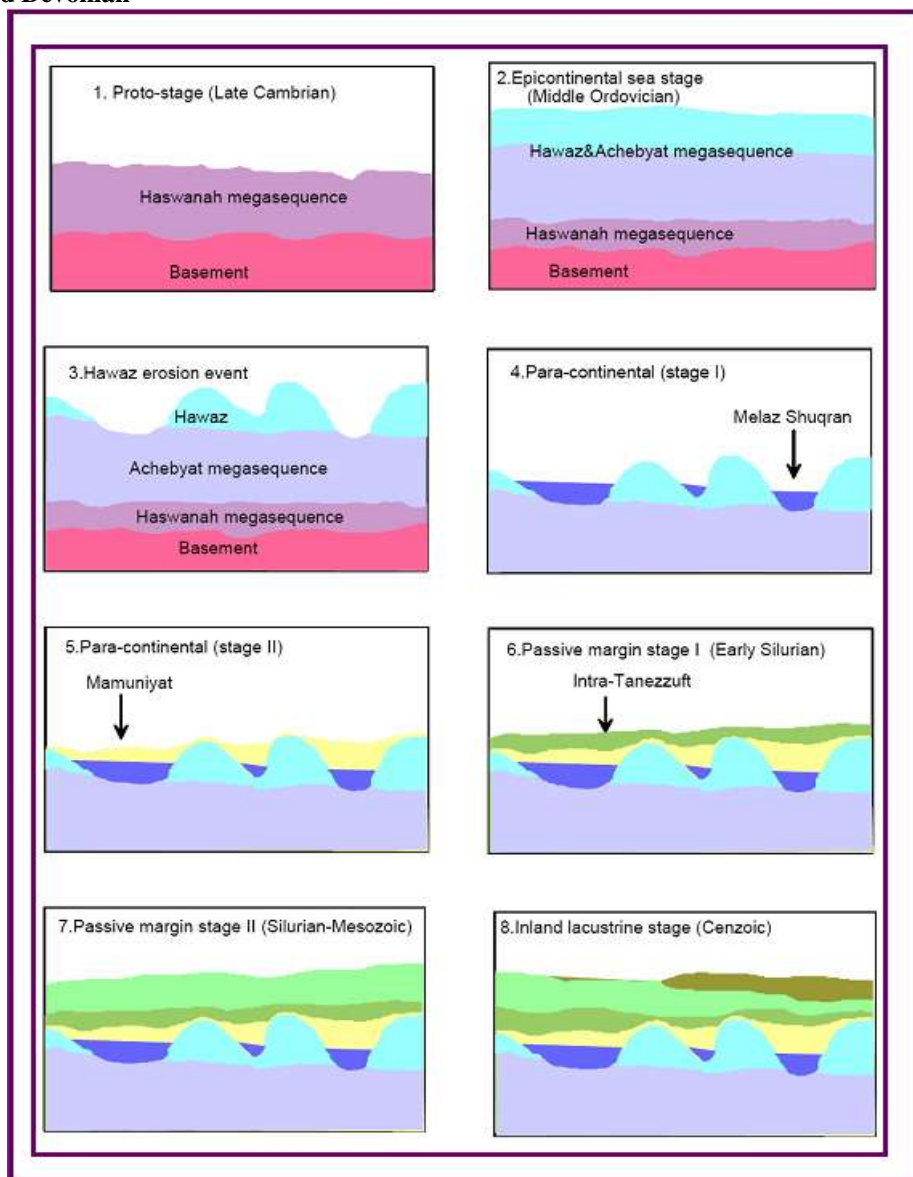
Silurian and Devonian

Figure 2: Tectono-stratiigraphic evolution of the Murzuq Basin (after Ghina and Alshabi, 2003).

The Silurian begins with the Tanezzuft Formation which overlies the Mamuniyat formation unconformably. This was deposited during marine transgression which spread from the north and reached across most of the North African margin. The lower part is composed of uranium rich hot shale of about 50 m considered to be the main source rock in the area. The overall thickness of this Formation is up to 800 m. Hallet 2002 reported a thickness ranging from 45 m to 320 m in the Murzuq basin. The Tanezzuft shales thin and become more arenaceous toward the northwest of the basin in the direction of Tripoli-Tibesti palaeohigh which clearly exerted an influence in the early Silurian Formation (Davidson *et al*., 2000). The age of the lower Tanezzuft is dated to be the early Llandovery. The Awaynat Wanin Formation of upper Devonian overlies the Tanezzuft Formation. This formation is composed of shales and sandstones often rich in ironstone, deposited in a littoral to shallow marine environment. The Akakus Formation which has been mapped in along the western flank of the Murzuq basin regarded as at least time equivalent of the of the Tanezzuft formation.

Devonian

The Devonian started with the Tadrat Formation. The Tadrat formation has been mapped along the western flank of the Murzuq basin from Tikiumit to the border of the Niger. In these areas the Tadrat formation is made up of lenticular sandstone bodies representing filled channels within a braided river. The environment of deposition ranges from subtidal to intertidal and continental. The thickness is about 140 m and the contact

with underlying Akakus Formation is distinctively unconformable (Hallet, 2002). The distribution of the Tadrat formation in the Murzuq basin has been greatly affected by the Devonian tectonism. The second megacycle in the Devonian resulted in the deposition of the Oan Kasa Formation, a marine transgressive sequence conformably overlying the massive sandstone of the Tadrat Formation. The Awayanat Wanin Formation capped the Devonian Oan Kasa which in turn is overlied by the Tahara formation.
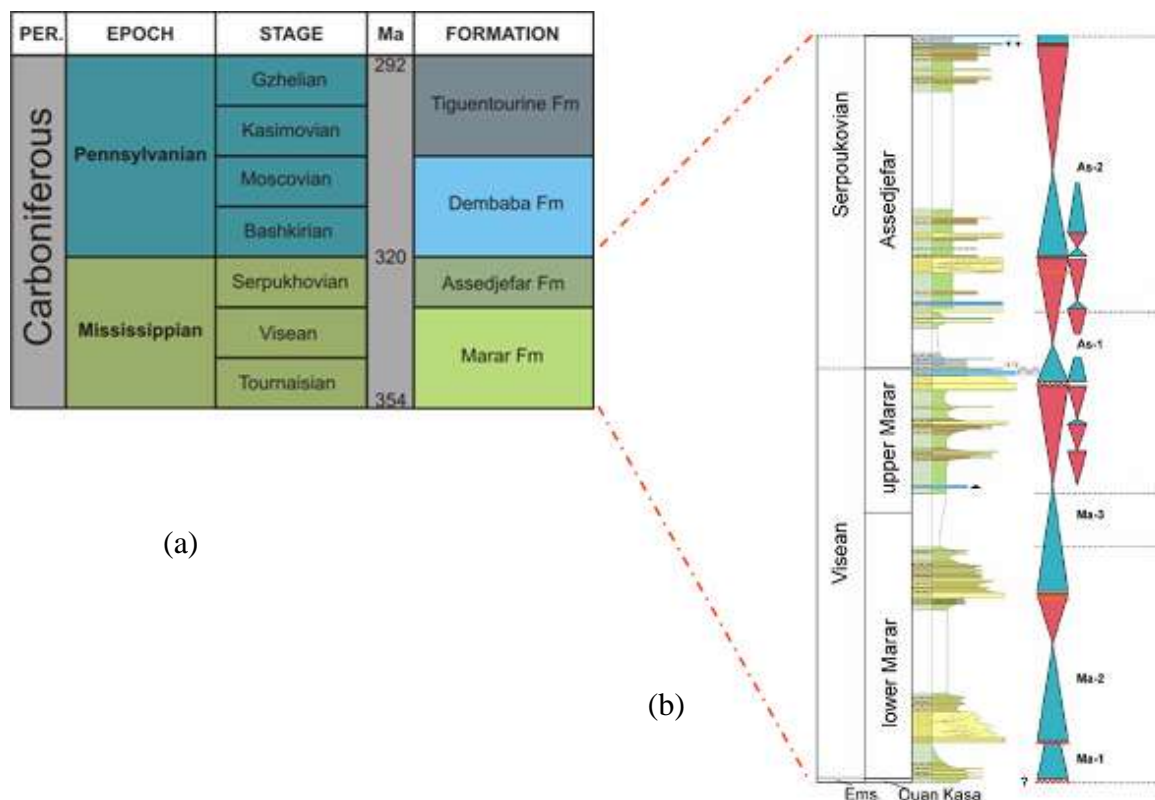

(a)

(b)

Figure 3: (a) Carboniferous stratigraphy of the Murzuq basin (b) showing sediment packages for Marar and Assedjefar Formations.

Carboniferous

The Carboniferous started with the Marar Formation which overlies the Tahara Formation which is in turn overlain by the Assedjefar Formation (Fig. 3). These Formations are composed of shales and sandstones assumed to be deposited in a shallow marine environment. The mainly fining upward sandstone may explain low energy condition. In the middle part of the Carboniferous, the Dembaba Formation was deposited above the Assedjefar Formation which is made up of shallow marine limestone, sandstone and grey shales in the northern part of Murzuq basin and lagoonal limestone and red shale in the south. The Dembaba Formation represents a transitional facies changing from the Palaeozoic marine condition to the Mesozoic continental condition. The Carboniferous was later uplifted and suffered from severe erosion and the uppermost Paleozoic sediments the lacustrine mudstone of the Tiguentourine Formation, exist only in patches. This erosion produced the Hercynian unconformity. There was no evidence of Permian deposits in the Murzuq basin. They were probably eroded or not deposited due to the regional uplift at the end of the Carboniferous.

Evidence from apatite fission track work, fluid inclusion data and shale studies indicates that the early Paleozoic rocks encountered in wells are not presently at their maximum burial depths, but have been subjected to significant uplift and cooling from that maximum depths reached (Glover, 1999).

Triassic, Cretaceous and Tertiary

During the Triassic, left-lateral movement of the African plate and opening of the Ligurian Tethys initiated extensional movements, which created slow intracratonic subsidence in the present Murzuq basin (Echikh and Sola, 2000). Uplift and erosion of the flanking Tihemboka and Tibesti highs during the Mesozoic resulted in the deposition of thick continental sand sequence in the present central parts of the basin. About 1700m of Mesozoic sediments were found overlying the Paleozoic deposits. It might have been thicker but some part have been eroded after the mid Cretaceous uplift (Austrian) and early Tertiary (Alpine) uplift. The Mesozoic deposits can be divided into fluvial sandstone and red mudstone of the Triassic to Jurassic

Zarzaitine/Taouratine formations and the fluvial sandstone, conglomerate and mudstone of the Jurassic/Lower Cretaceous Mesak formation.

III. Data Base and Methodology

The data used in this work include sixteen (16) thin sections prepared from outcrop samples collected in the Carboniferous Marar and Assedjefar Formations along the north western part of Murzuq basin by the North African Research Group members of the university of Manchester and well data (logs and biostratigraphic data) from 16 wells drilled through the Marar and Assedjefar Formations was provided by Woodside Energy. An outcrop log showing the units was obtained from previous fieldwork conducted.

Detailed correlation was done using PETREL software, a Schlumberger modeling tool. Combinations of log characters (Gamma ray, sonic, density, neutron, resistivity etc.) were studied and changes in log characters were used to correlate the wells.

Sequence boundaries and flooding surfaces were established based on the log characters to construct the sequence stratigraphic framework. Transgressive surface were determined from abrupt appearance of marine mudstone indicated by sudden increase in gamma ray log, maximum flooding surfaces were determined from the bow tie shape formed between gamma and sonic logs. Systems tracts were assigned objectively by their bounding surfaces. Sequence boundaries were estimated between the highstand systems tracts and the lowstand systems tracts bounded by their surfaces.

The N-S correlation is a stratigraphic correlation that has a datum at the base of the Marar Formation. The E-W correlation across strike has a datum at 100m depth to examine the present day structural configuration. The well correlation was used to determine the extent and thickness of units.

The polarizing microscope was used to study thin sections to identify detrital and authigenic composition of the rocks on thin sections. Detailed petrographic analysis was performed on 18 thin sections prepared from samples obtained from outcrop sections which were prepared after impregnation with blue epoxy in order to fill and highlight pore spaces. 5 thin sections from the lower part of the Assedjefar and 11 from Marar sampled in two locations of about 4.5 km apart within an incised valley (Unit B and C). Modal point count analysis was done on all thin sections to investigate mineralogy, grain size, pore type and pore volume (200 counts per thin section). In addition to the well logs core descriptions were used for creating lithological sections. Scanning electron microscope (SEM) JSM-6460 equipped with digital imaging was used to identify the types of clay and textural relation of some diagenetic minerals in selected samples after the thin section study. The samples were coated with a thin layer of gold and examined under an acceleration voltage of 15 kV and a beam of 20 nA.
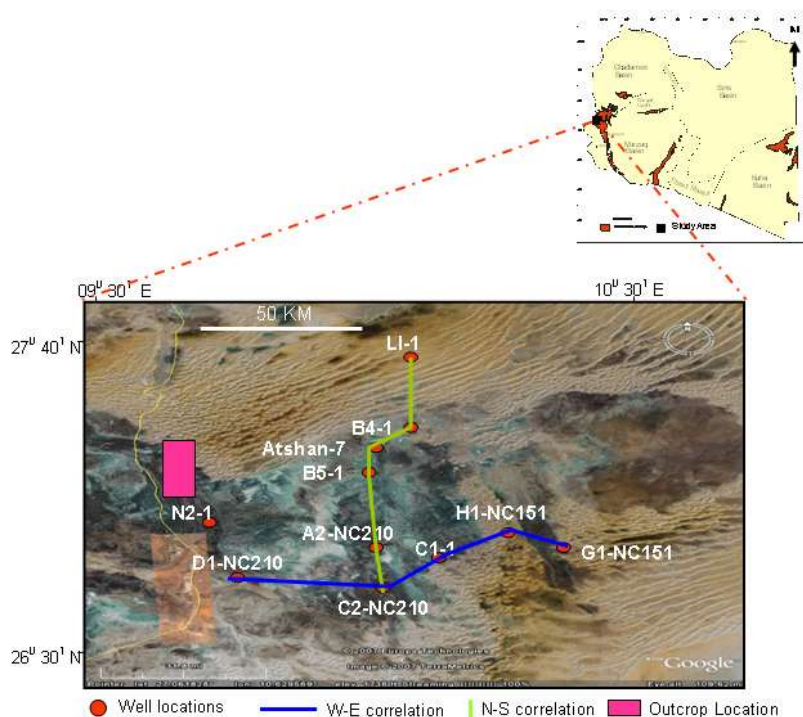

Figure 4: Showing well locations within the study area and cross section orientations.
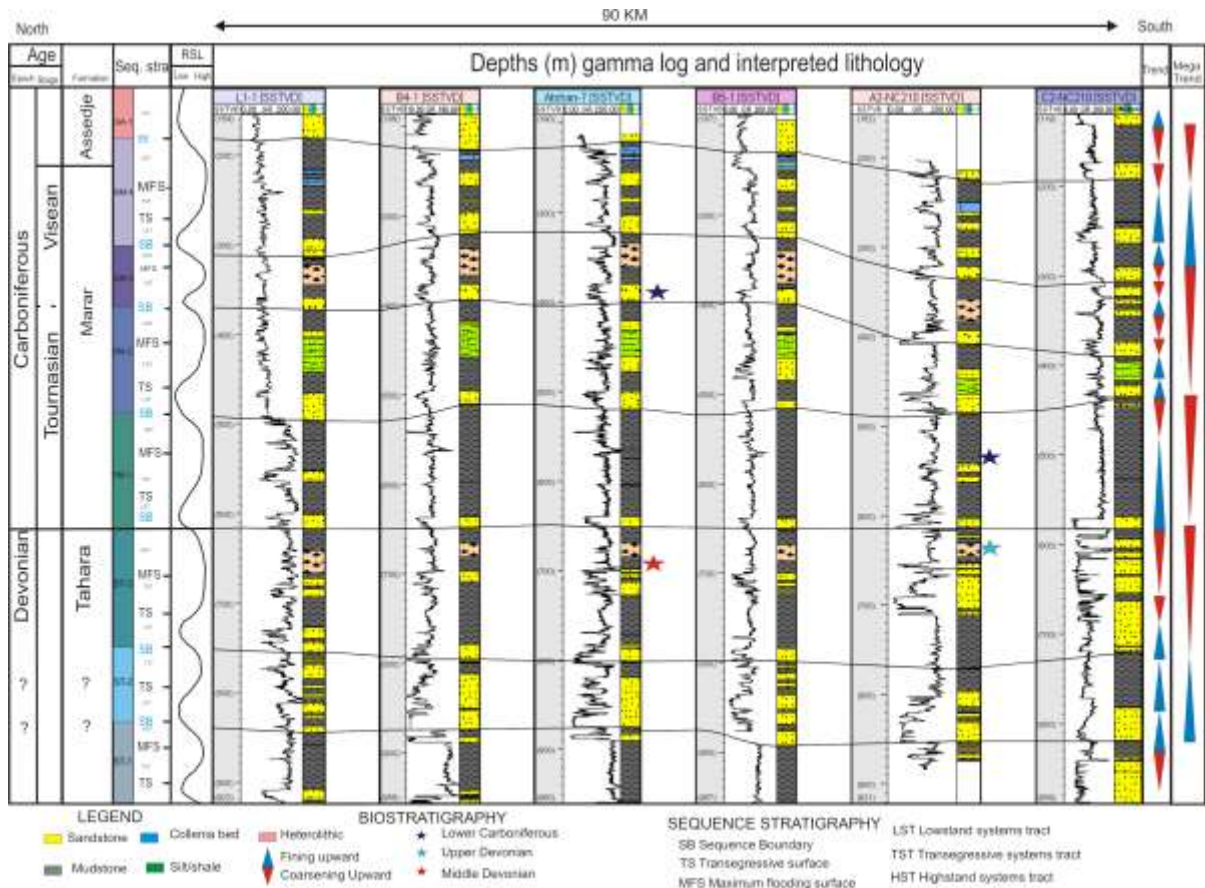
Figure 5: Showing North-South sequence stratigraphic framework and correlation pane of the study area.
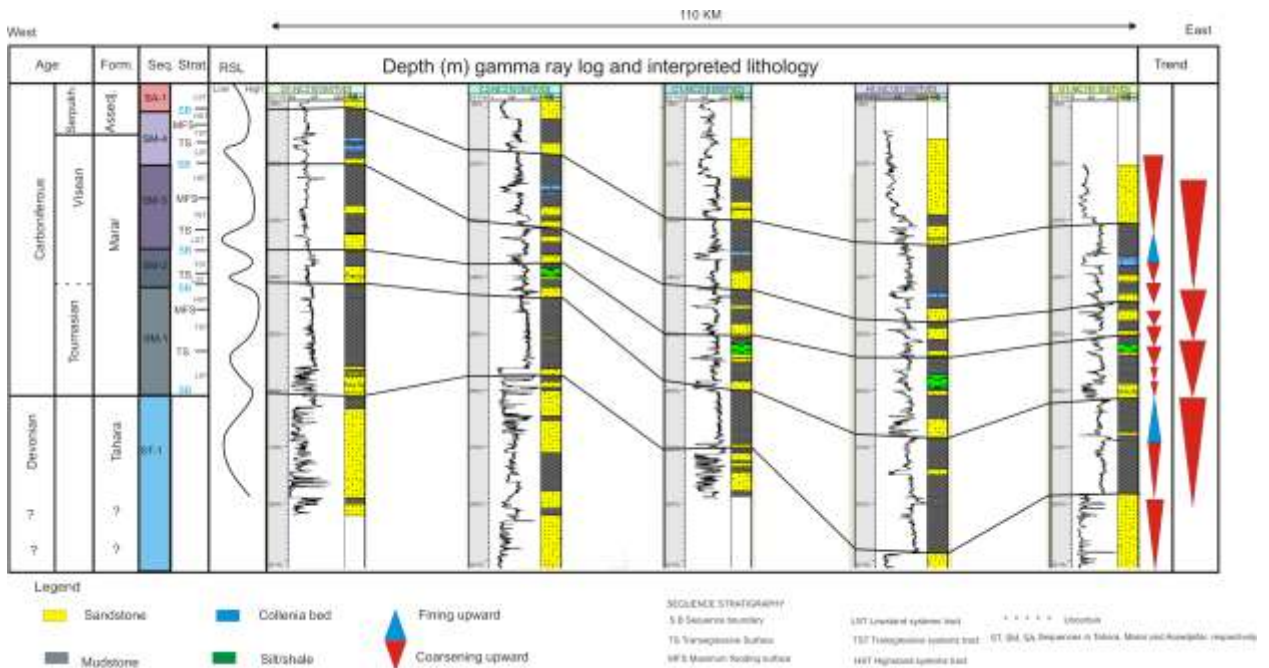

Figure 6: Showing West-East sequence stratigraphic framework and correlation panel.

IV.   Results

Sequence SM-1

Sequence SM-1 is bounded below by a sequence boundary which marks the contact between the Marar formation and the underlying Tahara formation (Fig. 6). This contact is marked by a sequence boundary identified from point of maximum regression indicated by the low gamma log value. This sequence maintains an average thickness of about 120 m in the N-S direction and 100 to 150 in the E-W direction. Three systems tracts have been identified: LST 1, TST 1 and HST 1. The LST 1 is identifiable throughout the N-S direction, but in the E-W direction it becomes a conformable correlative surface in the basinal section in wells H1-NC151 and G1-NC 151. The LST 1 is capped by transgressive surface that is correlatable in all the wells. The transgressive surface bounding the LST is identified based on the abrupt appearance of offshore marine mudstone. Above this surface, offshore mudstone were widely deposited probably, initially in a marginal marine environment, gradually becoming deeper water. An increase in marine influence leads to the deposition of TST 1 until the peak of the flood forming the maximum flooding surface (MFS) defined from maximum increase in off shore mud (high gamma peak and gamma sonic bow tie shape) which is clear in the N-S profile. HST 1 overlies the MFS 1 until the sequence boundary of the sequence SM-2.

Sequence SM-2

This sequence overlies the sequence boundary of Sequence SM-2. It has an average thickness of about 100 m in the north south direction (Fig. 5), thinning to less than 50 m in the extreme southern part. The thickness progressively increased from the west flank of the basin to the east, the more basinal side. Three systems tracts, LST 2, TST 2 and HST 2 have been identified in the N-S correlation while 2 were identified in the E-W correlation based on their bounding surfaces. The LST 2 is sandstone unit above the sequence boundary 2 (identified from point of maximum regression) with thickness decreasing toward the basinal side in the east-west direction (Figure 6), while near consistent thickness in the north-south direction. A widespread transgressive surface (marked by abrupt appearance of marine clay shown by increase in gamma log value) is evident throughout the area marked the top of the LST 2 and the base of TST 2 assumed to be deposited in a shallow marine condition. The TST 2 is a marine mudstone with about 10 m of tidal sandstone layer. The maximum flooding surface (identified from well developed offshore mudstone with highest gamma peak and the bow tie shape on sonic log) separated the TST 2 and HST 2 is well pronounced in the north-south profile. The HST 2 is characterized by siltstone mudstone intercalation, interpreted to be a turbidite like deposits shown by a serrated gamma response.

Sequence SM-3

Sequence SM-3 is bounded at the bottom by the sequence boundary SB 3 and at the top by the SB 4 identified from the point of maximum regression shown by drop in gamma value. This sequence is about 120 m thick at the western side (proximal) and reduced progressively to about 40 m in the eastern side (distal) in the east-west profile. In the north-south profile, a near constant thickness of about 70 m is maintained (Fig. 5). Two systems tracts have been recognized, LST 3, and HST 3. The LST is a low gamma sandstone unit of about 15 m thick at the proximal and thinned basinward to 10 m. The HST 3 separated from the LST 3 by a flooding surface is about 60 m in the north south profile and 120 m in the west to less than 50 m in the east as shown on the east-west profile, relatively thicker than in previous systems tracts and contains a transgressive sands reworked by waves or tide in the middle part. This unit is interpreted as heterolithic in the north-south profile but is clearly shown to be sandstone dominated in the east-west profile.
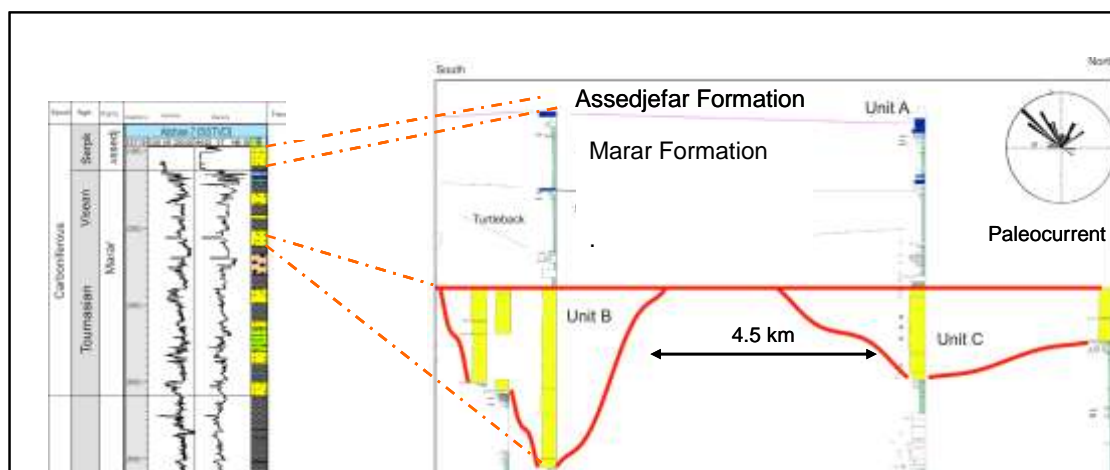
Figure 7: Well and outcrop correlation showing the horizons where studied samples were picked. Outcrop log from Laurent Petitpierre. For locations refer to Figure 3.

Sequence SM-4

This sequence is bounded below by SB 3 a regional regressive surface and above by sequence boundary of the sequence SA 1 in the lower part of Assedjefar formation (Figures 5 and 6). The sequence boundary here does not correspond to the formation boundary because of the conformable nature of the contacts between the Marar and Assedjefar formations. Three systems tracts were recognized in this sequence. The LST 4 is overlain by transgressive surface recognizable (from the abrupt appearance of marine mud shown by the increase in the gamma log value) in the whole area and TST 4 composed of marine mudstone. At the top of the TST 4 is the maximum flooding surface where the collenia bed was formed in a logoonal environment. The collenia bed is identified in most of the wells from neutron density cross plot throughout the area (Fig.5 and 6).

Assedjefar Formation

One sequence has been studied and described in this formation. Sequence SA-1 at the base of Assedjefar formation is not fully covered in most of the wells due to lack of well logs at that depth to establish that. Depositional sequence boundary of sequence SM-4 does not correspond with the formation boundary between the Marar and the Assedjefar formations (Fig. 5) because of the conformity between the two units.

Sequence SA-1

This sequence is not completely covered because of the limited well log information for that depth. However, in the east-west profile it can be seen that there is thick LST sandstone and that was the horizon where samples from unit A were collected.

Petrography

Petrographic data used were from three sandstone horizons herein classified as Sandstone Units A, B and C. Sandstone unit A is within a low stand systems tract about 30 meters thick and sandstone mudstone alternating beds at the lower most part of the Assedjefar formation (Figure 5). The unit lies above a collenia bed which separates from the Assedjefar from the Marar formation. From the well correlation (Figures 5 and 6) this unit seem to have wide lateral continuity. Sandstone unit B is about 20 meters thick and comprises fining upward sandstone interpreted to have been deposited in an incised lowstand systems tract of sequence SM-4 at the upper part of the Marar Formation. Sandstone unit C is about 20 m thick fining upward sequence in lowstand systems tract of sequence SM-4 of the Marar Formation at a distance of about 45 km away from unit B at a more distal location.

Detrital component

The sandstone in unit A are dominantly fine-grained, moderately to well sorted sub-arkoses (Fig. 7). Monocrystalline quartz range from 75.7-92.1; (averaging 83.9 vol. %) which is more abundant than polycrystalline quartz (4-19%, averaging 11%) and constitute the most abundant mineral constituents (Table 1). Feldspars range from 2.4 - 6.7%, averaging 4.6% by volume with mainly plagioclase, orthoclase and traces of microcline. The sands do not contain any lithic fragments, but traces of mica flakes (mainly showing a preferred orientation), an average of about 0.35% by volume. This unit contains abundant detrital clay fragments. Sandstones in this unit contain abundant calcite cement and show no porosity.

Large crystal of calcite cement occurs as intergranular cement filling pores. Calcite also occurs as tiny coatings around grains and as poikilotopic with grains floating in it. No quartz cementation was observed.

The sandstone in this unit does not show much effect of mechanical compaction because the mica flakes and the detrital muds do not show much deformation. Chemical compaction is shown by the pressure solutions (a grain to grain contact solution) around quartz grain. There is only trace of porosity in some samples while in most samples the porosity is completely obliterated by the calcite cements to around 5% in this unit.

The sandstone in unit B is dominantly fine to medium-grained, moderately to well sorted sub arkoses. Monocrystalline quartz range from 77.2 to 95.0% averaging 86.1 %) more abundant than polycrystalline quartz (5.5- 11.6% averaging 8.05%) constitute the most abundant mineral constituent (Table 1). Feldspar range from (2.0-8.3) averaging 5.15% mainly plagioclase and orthoclase (Table 1). No lithic fragments were identified but traces of mica flakes (average 3.5%) by volume. Detrital mud clast and authigenic clays are abundant.

Large crystals of calcite and sometime trace calcite are seen as replacement of detrital grains and intergranular cement filling large pores, and rarely as tiny grain coatings. The large calcites optically continuous, locally twinned and poikilotopically (Fig. 8A-D) enclosing the framework grains.
This sandstone unit does not show much evidence of mechanical compaction. This is because there is no major plastic deformation of the detrital mud clasts and the micas are pristine. Early formation of the calcite cement might have stopped stress on the mud clast. There is evidence of chemical pressure shown by the pressure solution around the quartz grains. Average porosity is about 5%.

The sandstone unit C is dominantly fine - grained, very well sorted (Fig. 10A and C) quartz arenite. Monocrystalline quartz range from 86.1-90.2 averaging 88.15%), more abundant than polycrystalline quartz (5.2-11.2% averaging 8.2%) constitute the most abundant mineral constituent. Feldspar range from (2.5-7.8%) averaging 3.4% mainly orthoclase. Rare lithic fragments averaging 0.25% were found no mica was recorded. No detrital mud clasts but authigenic clay mainly kaolinite Fig. 10B and D). Rare cement and has very high primary and dissolution porosity (Figure 10A and B).
The most important diagenetic component in this sample is the patches of kaolinite occurring as booklets and observed with the SEM (Fig. 10D). Traces of iron oxide occur as reddish brown cements within the pore spaces. The iron oxide seems to be engulfed by the kaolinite and therefore predates the kaolinite.
This unit show some degree of mechanical compaction shown by the sutured contacts of the grains. The unit show both primary intergranular porosity and mouldic macro pores ranging from 10 to 25%, average 15%.
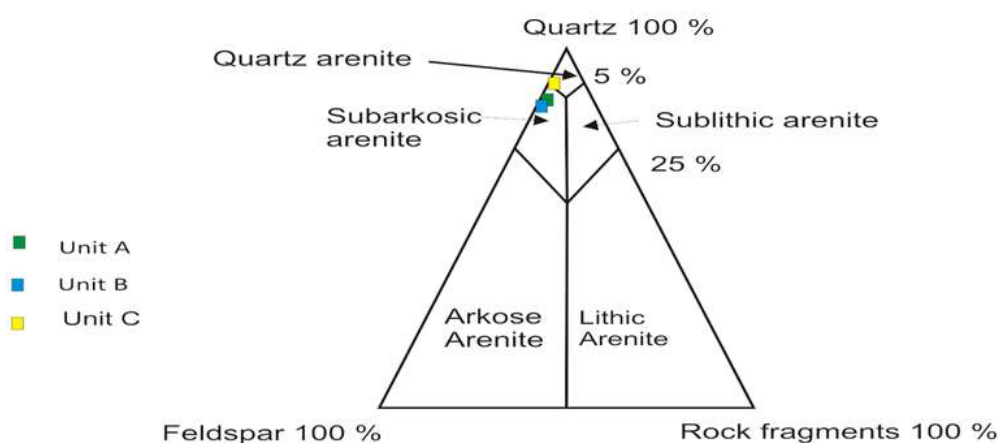

Figure 8: Classification of the sandstone studied using classification scheme of McBride (1963).

Table 1: Modal composition (maximum, minimum and average) of the sandstone samples from the three Units of the Marar and Assedjefar Formations.

Detrital minerals	Unit A sandstone			Unit B Sandstone			Unit C Sandstone		
	Min.	Max.	Average	Min.	Max.	Average	Min.	Max.	average
Monocrystalline quartz	75.7	92.1	83.9	77.2	95	86.1	86.1	90.2	88.15
Polycrystalline quartz	4	15	9.5	5.5	11.6	8.05	5.2	11.2	8.2
Feldspars	5	6.7	5.5	2	8.3	5.15	2.5	7.8	3.4
Lithic fragments	0	0	0	0	0	0	0	0.5	0.25
Micas	0	4	2	0	0.7	0.35	0	0.2	0.1
Mud clast	C	C	0	R	R	R	N	N	N
Heavy mineral	0	1.2	0.6	0	0.63	0.21	0	0	0
Quartz overgrowth	C	C	C	R	C	C	R	R	R
Pressure solution	VC	VC	VC	R	C	R/C	N	N	N
Illite	N	N	N	N	N	N	N	N	N
Kaolinite	C	C	C	C	C	C	R	C	R/C
Coarse crystalline calcite	C	C	C	C	C	C	N	N	N
Calcite inside grain	C	C	C	C	C	C	N	N	N
Microcrystalline calcite	C	C	C	C	C	C	N	N	N
Ferroan calcite	N	N	N	N	N	N	N	N	N
Silica cement	C	C	C	C	C	C	N	N	N
Iron oxide cement	VC	VC	N	R	C	C	C	C	C
Anhydrite	N	VC	N/VC	N	N	N	N	N	N
Porosity	0	10	5	0	10	5	10	25	16
Depositional porosity	0	5	2.5	0	0	5	5	10	7.5
Dissolution porosity	0	5	2.5	0	10	5	10	15	12.5

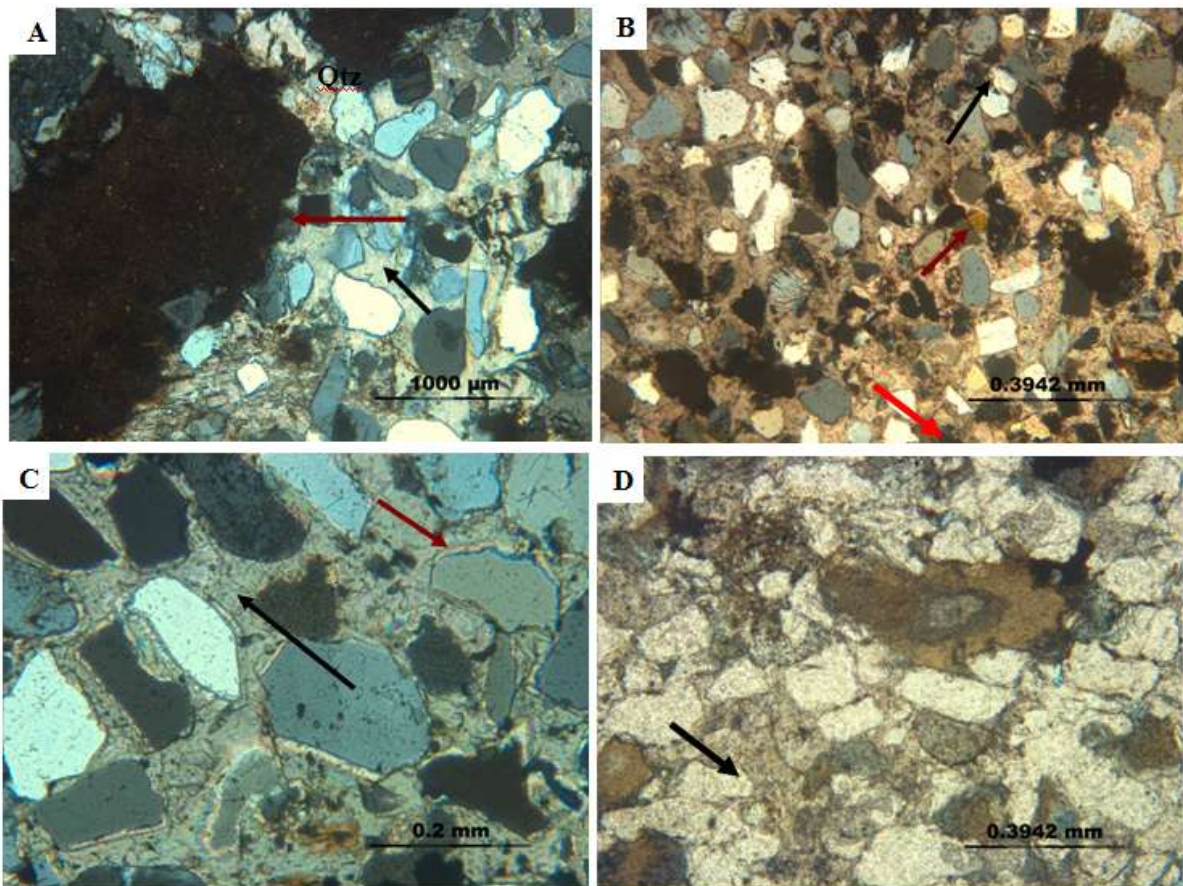N= None   R= Rare   C= Common   VC= Very common

Figure 8: (A) Photomicrograph showing a detrital mud clast (red arrow) and calcite cement filling large pores (black arrow) suggesting a near surface pre-compaction origin in unit A sandstone. (B) Photo micrograph showing barely deformed detrital mud (arrow) in unit A sandstone. (C) Showing coarse crystalline calcite cement (black arrow) and pressure solution rim (red arrow) around grains in unit A sandstone. (D) showing grain replacement calcite (black arrow) and glauconite (red arrow) in unit B sandstone.
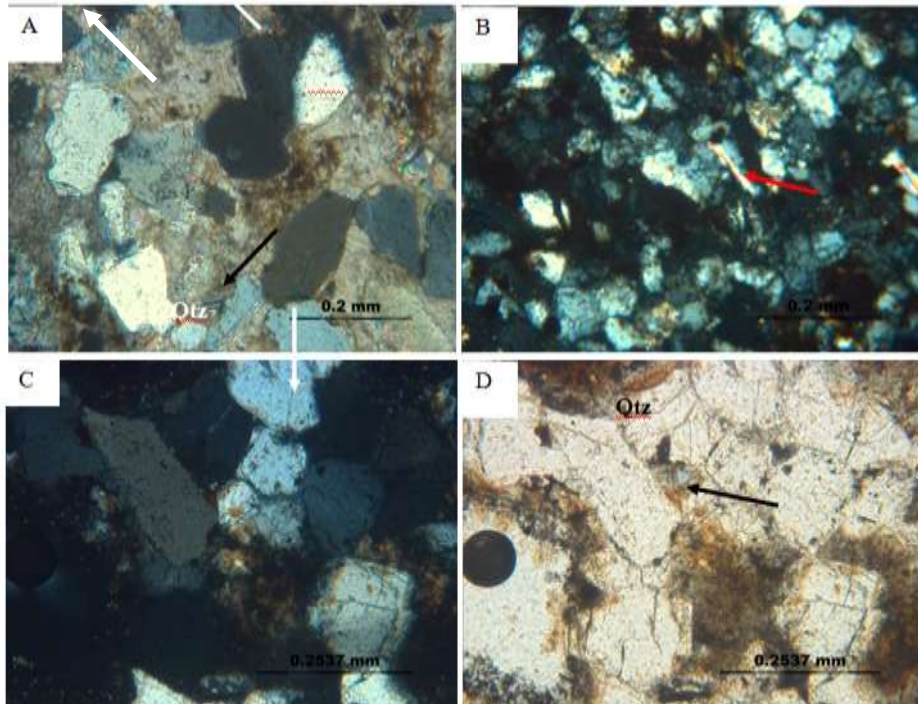
Figure 9: (A) Photomicrograph of (cross polar) showing poikilotopic calcite cement with no pore spaces (white arrow) and calcite replacement of detrital plagioclase feldspar in (black arrow) unit B sandstone. Subsequent dissolution of the replacement calcite can create secondary porosity. (B) showing undeformed muscovite flakes (red arrow) indicating less compaction effect in unit B sandstone. Photomicrographs (C) cross polar showing grain replacement calcite cement (D) plane polar showing traces of porosity (arrow).
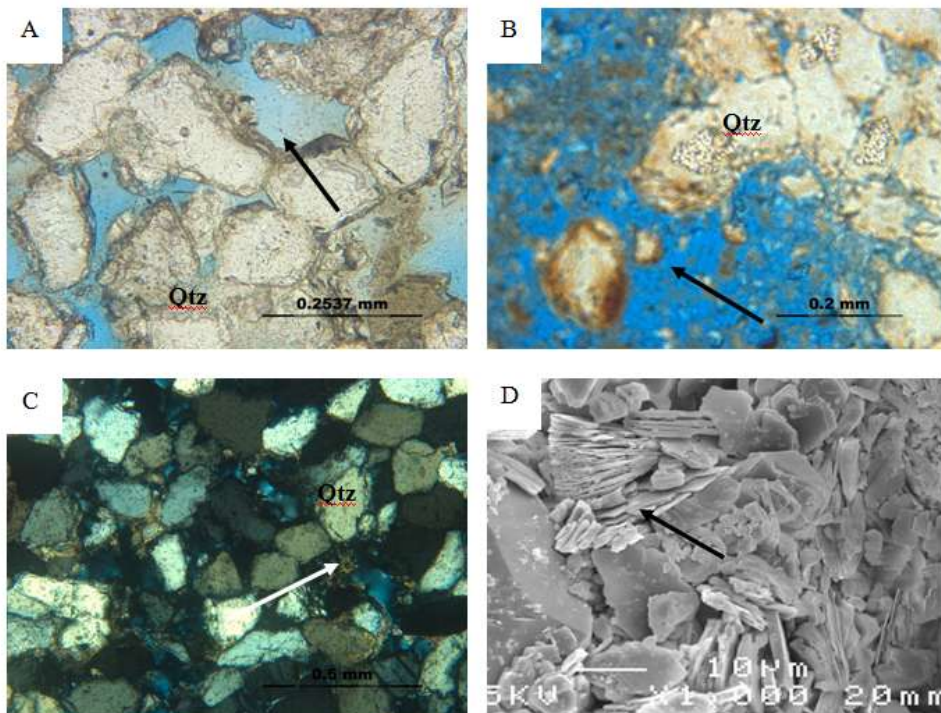

Figure 10: (A) Photomicrograph (plane polar) showing preserved primary interparticle porosity (blue stained). Detrital grains are mainly quartz in unit C sandstone. (B) showing oversize moldic porosity and barely visible clay rims passing through pores are indicative of dissolution of unstable grains in this sample in unit C sandstone.(C) Photomicrograph (cross polar) showing detrital quartz grains and pore spaces appearing black under cross polar in unit C sandstone. (D) SEM image showing vermicular kaolinite booklets composed of several plates (arrow) in Unit C sandstone

V. Discussion

Correlation and sequence stratigraphy

From the correlation of the wireline logs, the Marar formation has an average thickness of about 400 m (Figures 9 and 10) which is greater than 200-250 m reported by Jekovljevic (1984) for the east of Al-awayant, and less than the 650 m reported by Belhaj (2000) for the eastern part of the Murzuq basin. The N:G sand is higher in the eastern part than the western part of the Marar formation. In the N-S profile the net-to-gross (N:G) sand is higher to the south compared to the north. However sandstone thicknesses remain very similar.

Four sequences have been identified which show dominantly coarsening upward cycles similar to those described by Whitbread and Kelling (1982). The number of small scale cycles show slight variations depending on wells. These sequences are coarsening upward supporting the interpretation of the deltaic environment described by Belhaj (2000). The number of cycles is less than the 15 earlier described by Whitbread and Kelling in the Marar formation in the Ghadames Basin probably due to different orders of cyclicity used.

Alterations within sequence stratigraphy

Detrital quartz is the main constituent and framework grain in the Marar and Assedjefar sandstone units studied. The quartz grains in units A and B sandstones are corroded (Fig. 8A and 9A) and pressure solution is common. The feldspar grains are partially or completely replaced by calcite. The relic outlines of the original grains are discernable in some cases in the units A and B sandstones (Figure 8A). Other common detrital components is mud clasts. The mud clast is interpreted to be detrital based on the outline and geometric relationship with other grains which shows some degree of plastic deformation. The occurrence of abundant mudclast in sandstone units A and B at LST might have resulted in mechanical mobilization when the sea level is low and there is influx of detrital grains. Infiltrated clays in incised valley of LST sandstones were likely formed during a late stage of a LST when accommodation is progressively created in a fluvial like environment (Shanley and McCabe, 1994). The more abundant infiltrated clays in LST is attributed to high depositional permeability and percolation of surface waters rich in suspended mud into this sandstones (Mores and De Ross, 1990).

Diagenesis

Digenetic alterations in the Marar and the Assedjefar formations include calcite cementations, iron oxide cement precipitation, kaolinite formation, mechanical compaction and pressure solutions. However, the amount and nature of alteration varies within the sandstone units studied.

It is not possible to determine the time of the alterations since there is no burial history and isotopic composition, the textural relationship is used to determine the paragenetic stage of the calcite as early cementation.

Cementation

Calcite cementation is found in sandstone unit A and B both LST sandstones filling incised valleys. Calcite cements occur as intergranular cements filling large pore spaces in loosely packed sandstones (Fig. 8A), and as silicate grain alteration and coatings around the detrital grains (Fig. 9A). This indicates that there is more than one generation of cement. The poikilotopic calcite crystals which fill large pores between loosely packed sandstones commenced at the sea floor or within the eogenetic stage and the grain alteration calcite developed after burial with increase in temperature and pressure (Bukar et al, 2020).

The second generation of calcite in the studied sandstones is associated with pressure solution indication of chemical compaction which is not common during the early burial. Ketzer (2002) stated that the occurrence of coarse crystal of calcite cement in LST sandstone is due to the presence of carbonate bioclast which enhances nucleation sites and growth of carbonate cements. Therefore, amount and nature of organic matter is responsible for the cementation of the sandstones in unit A and B within LST. However, there was no indication of bioclast in the thin sections. The carbonate cement might have been derived from the adjacent carbonate beds (collenia).

Abundant quartz overgrowth shown by El-ghali (2005) in the LST and incised valley fill in the Mamuniyat and Melaz Shuqran formations of the Murzuq basin was not found in the LST sandstones of the Marar and Assedjefar formations studied here. The traces of iron oxide cement observed probably resulted from more extensive chemical weathering on landmass to provide detrital iron oxide and prolonged residence time of the sand layer under oxic condition (El-ghali, 2005) which is typical of LST sandstones.

Kaolinite

Kaolinite is present in form of patches in Sandstone unit C which show a very high porosity also in LST of sequence SM-4 of the Marar formation. The kaolinite could have been formed from the dissolution of

unstable grains. The dissolution of unstable framework grains such as feldspars, micas and mud intraclast and the formation of kaolinite in the unit C sandstone are attributed to near surface meteoric water influenced diagenesis (Meisler *et al.,* 1994, Morad *et al*., 2000, Ketzer *et al*., 2003, Worden *et al,* 2018). Evidence for early origin of kaolinite include the vermicular texture of the kaolinite, which has been suggested to occur soon after deposition (Wilkinson et al., 2004; Orsborne *et al*., 1994), and low compaction shown by the residual mud intraclast. This sandstone unit show high dissolution porosity. Porosity of sandstones in LST sub aerially exposed is commonly enhanced by dissolution of mica and feldspars accompanied by the formation of smaller volumes of kaolinite as a result of meteoric water percolation (Meisler *et al*., 1984). Kaolinite which is probably formed from the meteoric water dissolution of labile grains (feldspars and micas) is also stable in acidic waters.

Compaction and porosity

The Marar and Assedjefar formation sandstone show minor effect of mechanical compaction. The sandstones unit A and B show chemical compaction (pressure solution). The low evidence of the mechanical compaction is due to early cementation. Thin section porosity in sandstone units A and B is very low (less than 5%). Unit C sandstone has intergranular and moldic macropores. The intergranular porosity is of primary depositional origin and occurs within quartz grains with minor kaolinites. The moldic macropores are dissolution pores spaces formed from dissolution of the grain framework as a result of meteoric water attack. The present of the kaolinite does not have much effect on the porosity of the sandstone.

Reservoir quality is defined as the amounts of porosity and permeability, and its connectivity which can be a function of many controls (Meisler et al., 1994), including the depositional controls on grain size and sorting and the diagenetic control of cementation and compaction. Secondary porosity is sometime beneficial to reservoirs since most of it is redistribution porosity whereby the material from dissolved minerals is reprecipitated as cements elsewhere. The main controls on the reservoir quality of sandstone units studied are the calcite cement and total clay (detrital and diagenetic) content. The effect of compaction is not severe as the grain contacts are not sutured. This is contrary to the work of Mansurg (2007) which stated that compaction is more important in porosity destruction than cementation in LST sandstones due to the abundance of ductile grains.

Diagenetic alterations especially cement precipitation and the abundance of the mud intraclast has had an impact on the porosity distribution and thus reservoir quality. The mechanically infiltrated mudstone clast in sandstone units A and B will result in formation of baffles or barriers to fluid flow if they have lateral extension. The effect of the clay intraclast depends on the distribution of the clay. Mudstone intraclast distributed as structural clay as part of the frame work does not affect porosity and horizontal permeability as dispersed or lamination clay does (Stocks, 2004). Sandstone unit C Marar formation has very good porosity and permeability because of the grain dissolution. This is regarded as having good reservoir quality. Sandstone units A and B have no good porosity and are therefore poor reservoirs.

VI. Conclusion

Four coarsening upward sequences deposited in a deltaic environment have been identified. The sequences maintain fairly constant thicknesses in N-S direction and become thicker in the eastern part in the E-W direction. Net to gross is higher at the eastern and the southern parts of the studied area. The sandstones are arkoses in units A and B and quartz arenites in unit C.

The Unit A and B sandstones are highly cemented by early diagenetic calcite while the sandstone in unit C is porous and exhibits meteoric water dissolution which has enhanced the pore space.

The main sequence stratigraphic controls on the distribution and diagenetic alterations are composition of detrital influx, water chemistry, probably the type of adjacent lithology and position on the depositional slope.
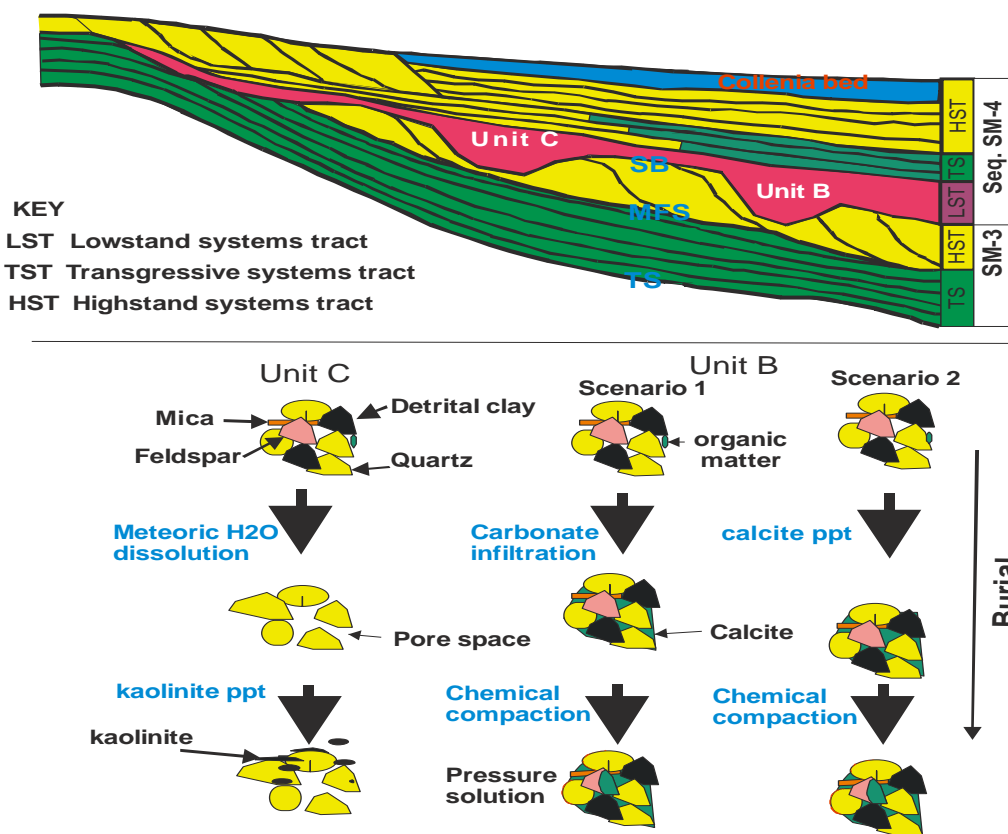
Figure 11: Diagenetic model of Sandstones Units B and C. Sandstone Unit B has scenario 1 in which the calcite is sourced from infiltrated carbonate bed (collenia) above and scenario 2 is precipitation of calcite from depositional organic matter.

Among the sandstone units studied, Units A and B have high proportion of calcite cement, mud intraclast and low porosity, while Unit C sandstone has no cement, high porosity, but it does contain kaolinite.

Units A and B are poor reservoirs while unit C is a good reservoir for hydrocarbon accumulation.

Prediction of spatial distribution of and resulting reservoir quality within the sequence stratigraphic framework is a viable tool but not without some limitations. Sandstones units B and C within an incised valley of the same LST of sequence SM-4 about 45 km apart gave contrasting porosities and therefore different reservoir properties.

References

[1]. Haq, B. U., Hardenbol, J., and Vail, P. R., (1987). Chronology of fluctuating sea-level since the Triassic. Science **235,** 1156-1166.
[2]. Van Wagoner, J. C., Mitchum, R. M., Campion, K. M., Rahmanian, V. D., (1990). Siliciclastic sequence stratigraphy in well logs, cores, and outcrops: concepts for high resolution to correlation of time and facies. American Association of Petroleum Geologists Bulletin. Methods in Exploration, Series **7,** 55p.
[3]. Morad, S., J. M., De Ross, F., (2000). Spatial and temporal distribution of digenetic alterations in silisiclastitc rocks; Implication for mass transfer in sedimentary basins, Sedimentology', **47**, 95-120.
[4]. Ketzer, J. M., Morad, S. and Amorosi, A., (2003). Predictive diagenetic clay mineral distribution in siliciclastic rocks within a sequence stratigraphic framework. In: H. Worden Riachad and S. Morad, Editors, Clay mineral cements in sandstones, International Association of Sedimentologist, (Special Publication) **34**, 42-59.
[5]. Echikh, J. and Sola, M. A., (2000). Geology and hydrocarbon occurrences in Murzuq Basin, SW Libya. In Sola, M. A.; Worsely, D. (Eds), Geological exploration in Murzuq Basin. Elsvier, Amsterdam, 295-320.
[6]. Klitzsch, E., (1971). Klitzsch, E., (1971). The structural development of parts of North Africa since Cambrian time. In: Gray, C. (ed.) Symposium on the Geology of Libya, Tripoli. 253–262. University of Libya.
[7]. Hallett, D., (2002). Petroleum Geology of Libya. Elsevier science B. V. 50.
[8]. Ketzer, J. M., Morad, S., and Al-Aasm, S., (2002). Distribution of diagenetic alterations in fluvial, deltaic, and shallow marine sandstones within a sequence stratigraphic framework: Evidence from the Mullaghmore Formation (Carboniferous), NW Ireland. Journal of Sedimentary Research, **71,** 760-774.
[9]. Vos, R. G., (1981). Sedimentology of an Ordovician fan delta complex, western Libya. Sedimentary Geology, **29,** 153-170.
[10]. Abugares, Y. I., and Remaekers. P., 1993. Short notes and guide book on Paleozoic geology of the Ghart area, SW Libya, Fieldtrip October 14-17, 1993. Earth Science Society of Libya. Interprint Ltd., Malta 84p.
[11]. Davidson, L., Beswatherick, S., Craig, J., Eales, M., Fisher, A., Himmali, A., Jho, J., Mejrab, B., Smart, J., (2000). The structure, stratigraphy and petroleum geology of the Murzuq Basin, SW Libya, In Sola, M. A.; Worsely, D. (Eds), Geological exploration in Murzuq Basin. Elsvier, Amsterdam, 295-320.

[12]. Smart, J., (2000). Seismic exploration of depositional processes in the Ordovician succession of Murzuq Basin SW Libya. In: M. A. Sola and D. Worsely (eds), Geological Exploration of Murzuq Basin. Elsevier, Amsterdam, 397-415.

[13]. Glover, T., Adamson, K., Whittington, R., Fitches, B. and Craig, T., (1999). Evidence for soft sediment deposition – the Duwayagash side of the Gargaf Arch, central Libya. In: M. A. Sola and D. Worsely (eds), Geological Exploration of Murzuq Basin. Elsevier, Amsterdam, p 417-430.

[14]. Mcbride, E. F., (1963). A classification of common sandstones. Journal of sedimentary Petrology, **33**, 664-669.

[15]. Jeklvljevic, Z., (1948). Geological map of Libya, 1:250,000 sheet Al-awayanat NG 32-12- Explanatory booklets.

[16]. Belhaj, F., (2000). Carboniferous and Devonian stratigraphy-the Marar and Tardrat reservoir, Ghademis Basin Libya. In: M. A. Sola and D. Worsely (eds), Geological Exploration of Murzuq Basin. Elsevier, Amsterdam, 117-142.

[17]. Shanley, P. and McCabe, J. (19940 perspective on the sequence stratigraphy of the continental strata. American association of Petroleum Geologist 78, 544-568.

[18]. Mores, M. A. S.and De Ros, L. F., (1990). Infiltrated clay in fluvial Jurassic sandstones of Reconcovo Basin, northeastern Brazil. Journal of Sedimentary Petrology, **60**, 809- 819.

[19]. Bukar, M., Worden, R. H., Shettima, B. and Shell, P. (2021). Diagenesis and its control on reservoir quality of the Tambar Oil Field, Norwegian North Sea. Energy Geoscinece, 2, 10-31

[20]. El-ghali, M. A. K., (2005). Depositional environment and sequence stratigraphy of paralic glacial, paraglacial and postglacial Upper Ordovician silisiclastic deposits in the Murzuq basin, SW Libya**.** Sedimentology **177**, 145-173.

[21]. Meisler, H. Leahy, P. P. and Knobel, L. L. (1984) Effect of rustatic sea-level changes on salt water-fresh water in the North Atlantic Coast Plain. United State Geological Survey Water Supply Paper **2255** , 27p

[22]. Worden, R. H., Bukar, M and Shell P. (2018). The effect of oil emplacement in quartz cementation. American Association of Petroleum Geologists Bulletin. 102 (1), 49-75.

[23]. Osborne, M. Haszeldine, R. S. and Fallick, A. E. (1994) Variation in kaolin morphology with growth temperature in isotopically mixed pore-fluids. Brent Group, UK North Sea, Clay Mineral **29**, 591-608.

[24]. Mansurg, H. (2007). Diagenesis and reservoir quality evolution. Digital comprehensive summaries of Upsala Desertations from the Faculty of Science and technology, 279.

[25]. Ghina, S. and Ashaibi, A., (2003) C0ntribution to the stratigraphy of Murzuq Basin, SW Libya, from the view of NC-115 data. American Association of Petroleum Geologists Hardenberg conference, February 18-30, 2003 Algiers, Algeria.

[26]. Stocks, A. (2004) Formation evaluation. Petroleum Geoscience lecture notes, University of Manchester.